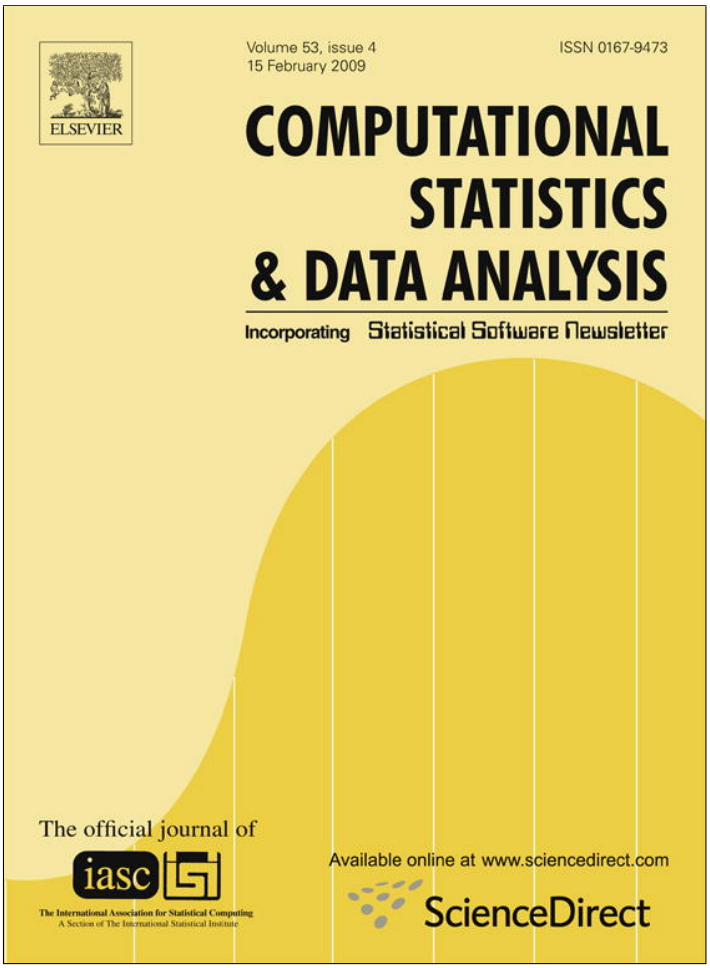

Computational Statistics and Data Analysis 53 (2009) 1440–1448

Contents lists available at ScienceDirect

Computational Statistics and Data Analysis

journal homepage: www.elsevier.com/locate/csda

Control chart based on likelihood ratio for monitoring linear profiles

Jiujun Zhang [a,b], Zhonghua Li [b], Zhaojun Wang [b,*]

[a] Department of Mathematics, Liaoning University, Shenyang 110036, PR China

[b] LPMC and School of Mathematical Sciences, Nankai University, Tianjin 300071, PR China

ARTICLE INFO

Article history:
Received 5 July 2008
Received in revised form 25 November 2008
Accepted 15 December 2008
Available online 24 December 2008

ABSTRACT

A control chart based on the likelihood ratio is proposed for monitoring the linear profiles. The new chart which integrates the EWMA procedure can detect shifts in either the intercept or the slope or the standard deviation, or simultaneously by a single chart which is different from other control charts in literature for linear profiles. The results by Monte Carlo simulation show that our approach has good performance across a wide range of possible shifts. We show that the new method has competitive performance relative to other methods in literature in terms of ARL, and another feature of the new chart is that it can be easily designed. The application of our proposed method is illustrated by a real data example from an optical imaging system.

1. Introduction

In most statistical process control (SPC) applications, it is assumed that the quality of a process or product can be adequately represented by the distribution of a univariate quality characteristic, or by the general multivariate distribution of a vector consisting of several quality characteristics. In many practical situations, however, the quality of process or product is characterized and summarized better by a relationship between a response variable and one or more explanatory variables. In particular, there has been recent interest in monitoring processes characterized by simple linear regression profiles. Most of the studies conducted in the monitoring of such linear profiles have been motivated by calibration applications. Mestek et al. (1994), Stover and Brill (1998), Lawless et al. (1999) and Kang and Albin (2000) presented some practical applications in industrial engineering.

Process monitoring mainly using control charts can be seen as a two stage process-Phase I and Phase II (Woodall, 2000). The goal in Phase I is to evaluate the stability of the process and, after dealing with any assignable causes, to estimate the in-control values of the process parameters. In contrast, the main concern in the analysis of Phase II is to quickly detect shifts in the process from the in-control parameter values estimated in Phase I. Different types of statistical methods are appropriate for the two phases, with each type requiring different measures of statistical performance. In Phase I it is important to assess the rate of false signals of a control chart with a given type one error determined by practitioners. In Phase II, the emphasis is on detecting process changes as quickly as possible. That is usually measured by parameters of the run length distribution, where the run length is the number of samples taken before an out-of-control signal is given.

Most of the literature concerned with profile monitoring deals with the Phase II analysis of linear profiles when the underlying in-control model parameters are assumed to be known. Kang and Albin (2000) proposed two control charts for Phase II monitoring of linear profiles. One of these is a multivariate T^2 chart and the other is a combination of an exponentially weighted moving average (EWMA) chart and a range (R) chart. Kim et al. (2003) proposed transforming the x values to achieve an average coded value of zero, and a method based on the combination of three EWMA charts was proposed for detecting a shift in the intercept, the slope and the standard deviation. Gupta et al. (2006) compared the performance of

* Corresponding author.
E-mail addresses: jiujunzhang2000@yahoo.com.cn (J. Zhang), 0210008@mail.nankai.edu.cn (Z. Li), zjwang@nankai.edu.cn (Z. Wang).

0167-9473/$ – see front matter © 2008 Elsevier B.V. All rights reserved.
doi:10.1016/j.csda.2008.12.002

two phase II monitoring schemes for linear profiles, the control charting schemes proposed by Croarkin and Varner (1982) and Kim et al. (2003). The simulation study shows that the Croarkin and Varner (1982) method performed poorly compared to the combined control charting scheme of Kim et al. (2003). Recently, Zou et al. (2007) proposed a novel multivariate exponentially weighted moving average scheme for monitoring general linear profiles. They showed that their approach performed better than Kim et al. (2003) for small and moderate shifts.

For Phase I analysis, Kim et al. (2003) suggested replacing the Phase II EWMA charts with Shewhart charts. Mahmoud and Woodall (2004) studied the Phase I method for monitoring the linear profiles. Mahmoud et al. (2007) proposed a change-point method, based on the likelihood ratio statistics, to detect sustained changes in a linear profile data set in Phase I. They concluded that to protect against both kinds of changes, sustained and randomly occurring unsustained shifts, one could employ the change-point method in conjunction with the methods proposed by Mahmoud and Woodall (2004). A discussion about the problems in monitoring linear profiles is given in Woodall et al. (2004). Recently, Jensen et al. (2008) proposed the use of linear mixed models to monitor the linear profiles in order to account for any correlation structure within a profile and Williams et al. (2007) extended the use of the T^2 control chart to monitor the coefficients resulting from a parametric nonlinear regression model fit to profile data.

Based on the generalized likelihood ratio test, we propose a new method to detect shifts in the linear profile. Moreover, the comparisons among our proposed method, the multivariate exponentially weighted moving average scheme of Zou et al. (2007) (henceforth referred to as MEWMA) and the combined control chart of Kim et al. (2003) (henceforth referred to as KMW) are carried out in this paper. We compare these three methods in terms of ARL performance under sustained shifts of different magnitudes in the intercept, slope and the error variance.

The rest of this paper is organized as follows. In Section 2, we review the existing two competitive monitoring methods, the MEWMA and KMW charts and present our proposed scheme. We present the proposed chart with VSI feature in Section 3 and compare the monitoring performance of the proposed scheme with those two methods in Section 4. In Section 5, the application of our proposed method is illustrated by a real data example from an optical imaging system. We summarize this paper in Section 6 with some conclusions.

2. Control chart for linear profiles

Denote by $\{(x_i, y_{ij}),\ i = 1, 2, \ldots, n\}$ the jth random sample collected over time. When the process is in control, the relationship between the response and explanatory variables is assumed to be

$$y_{ij} = A_0 + A_1 x_i + \varepsilon_{ij}, \quad i = 1, 2, \ldots, n, \tag{1}$$

where the ε_{ij}/σ are independently identically distributed (i.i.d) as a standard normal random variable, and the explanatory variable x is assumed to be fixed at n values. This is usually the case in the practical applications and is consistent with Kang and Albin (2000), Kim et al. (2003) and Mahmoud and Woodall (2004). In this paper, we consider the Phase II case in which the in-control (IC) values of the parameters A_0, A_1 and σ^2 are assumed to be known.

2.1. The existing work

The KMW chart (Kim et al., 2003): In Kim et al. (2003), using the coded explanatory values, they obtained the following alternative form of the underlying model

$$y_{ij} = B_0 + B_1 x_i^* + \varepsilon_{ij}, \quad i = 1, 2, \ldots, n, \tag{2}$$

where $B_0 = A_0 + A_1\bar{x}$, $B_1 = A_1$, $x_i^* = x_i - \bar{x}$ and $\bar{x} = \frac{1}{n}\sum_{i=1}^{n} x_i$. For the jth sample, the least square estimators for B_0, B_1 and σ^2 are

$$b_{0j} = \bar{y}_j, \quad b_{1j} = \frac{S_{xy(j)}}{S_{xx}}, \quad MSE_j = \frac{1}{n-2}\sum_{i=1}^{n}(y_{ij} - b_{1j}x_i^* - b_{0j})^2,$$

where $\bar{y}_j = \frac{1}{n}\sum_{i=1}^{n} y_{ij}$, $S_{xx} = \sum_{i=1}^{n}(x_i - \bar{x})^2$ and $S_{xy(j)} = \sum_{i=1}^{n}(x_i - \bar{x})y_{ij}$. Note that these three estimators are independent. Thus, they proposed to use three EWMA charts (EWMA_I, EWMA_S, EWMA_E) to detect if the Y-intercept (B_0), slope (B_1) and standard deviation (σ) had changed, respectively. They are

$$\begin{aligned}
&\text{EWMA}_I(j) = \theta b_{0j} + (1-\theta)\text{EWMA}_I(j-1),\\
&\text{EWMA}_S(j) = \theta b_{1j} + (1-\theta)\text{EWMA}_S(j-1),\\
&\text{EWMA}_E(j) = \max\left\{\theta \ln(MSE_j) + (1-\theta)\text{EWMA}_E(j-1), \ln(\sigma^2)\right\},
\end{aligned}$$

where $\text{EWMA}_I(0) = B_0$, $\text{EWMA}_S(0) = B_1$, $\text{EWMA}_E(0) = \ln(\sigma^2)$ and θ is a smoothing constant. The three EWMA charts are used jointly, with the combination of charts signaling with the first chart to signal. Their ARL comparisons show that the three EWMA charts are more effective than the methods of Kang and Albin (2000) in terms of ARL in Phase II for detecting sustained shifts in either Y-intercept or slope or increases in the error variance. In particular, the three EWMA charts are

more effective in detecting shifts in the slope of the line when the average Y-value does not change — i.e. the shifts in parameter B_1 of Eq. (2). Also, their method seems much more interpretable.

The MEWMA chart (Zou et al., 2007): In Zou et al. (2007), they considered the general linear profile model. Assume that for the jth random sample collected over time, they have the observations $(\mathbf{X}_j, \mathbf{Y}_j)$, where $\mathbf{Y}_j$ is n_j-variate vector and $\mathbf{X}_j$ is a $n_j \times p (n_j > p)$ matrix. When the process is in-control, the underlying model is

$$\mathbf{Y}_j = \mathbf{X}_j\vec{\beta} + \vec{\varepsilon}_j, \tag{3}$$

where $\vec{\beta} = (\beta^{(1)}, \beta^{(2)} \ldots, \beta^{(p)})$ is the p-dimensional coefficient vector and the $\vec{\varepsilon}_j's$ are i.i.d as an n_j-variate multivariate normal random vector with mean $\vec{0}$ and $\sigma^2\mathbf{I}$ covariance matrix. Without loss of generality, suppose that $\mathbf{X}_j$ is of form $(\mathbf{1}, \mathbf{X}_j^*)$, where $\mathbf{X}_j^*$ is orthogonal to $\mathbf{1}$ and $\mathbf{1}$ is a n_j-variate vector of all 1′s. The $n_j's$ are equal and $\mathbf{X}_j$ is assumed to be fixed for different j, denoted as n and $\mathbf{X}$, respectively. Following the notation in (3), they define

$$\mathbf{Z}_j(\vec{\beta}) = (\vec{\hat{\beta}}_j - \vec{\beta})/\sigma,$$

and

$$Z_j(\sigma) = \Phi^{-1}\{F((n-p)\widehat{\sigma}_j^2; n-p)\},$$

where $\vec{\hat{\beta}}_j = (\mathbf{X}'\mathbf{X})^{-1}\mathbf{X}'\mathbf{Y}_j, \widehat{\sigma}_j^2 = \frac{1}{n-p}(\mathbf{Y}_j - \mathbf{X}\vec{\hat{\beta}}_j)'(\mathbf{Y}_j - \mathbf{X}\vec{\hat{\beta}}_j)$, Φ^{-1} is the inverse of the standard normal cumulative distribution function, and $F(\cdot; \nu)$ is the chi-squared distribution function with ν degrees of freedom. Denote $\mathbf{Z}_j$ by $(\mathbf{Z}_j'(\vec{\hat{\beta}}), Z_j(\sigma)')$, which is a $(p+1)$-variate random vector. When the process is in-control, the vector is multivariate normally distributed with mean $\vec{0}$ and covariance matrix $\mathbf{\Sigma} = \begin{pmatrix} (\mathbf{X}'\mathbf{X})^{-1} & \mathbf{0} \\ \mathbf{0} & 1 \end{pmatrix}$.

The EWMA charting statistic is defined as

$$\mathbf{W}_j = \lambda\mathbf{Z}_j + (1-\lambda)\mathbf{W}_{j-1}, j = 1, 2, \ldots, \tag{4}$$

where $\mathbf{W}_0$ is a $(p+1)$-dimensional starting vector and λ is a smoothing constant parameter. The chart signals when

$$U_j = \mathbf{W}_j'\mathbf{\Sigma}^{-1}\mathbf{W}_j > L\frac{\lambda}{2-\lambda}, \tag{5}$$

where $L > 0$ is chosen to achieve a specified IC ARL. This control scheme can be deemed a special application of MEWMA charts. The MEWMA chart was first proposed by Lowry et al. (1992); the design of MEWMA chart was investigated by Prabhu and Runger (1997).

2.2. Our proposed methodology

We consider model (2) and assume that $\sigma^2 = 1$ when the process is in-control, without loss of generality. For the tth random sample collected over time, we have observations (x_i^*, y_{it}), $i = 1, 2, \ldots, n$. If the coded model at time t is assumed to be

$$y_{it} = b_0^{(t)} + b_1^{(t)}x_{it}^* + \varepsilon_{it},$$

then we consider the following hypothesis test

$$H_0 : b_0^{(t)} = B_0, \quad b_1^{(t)} = B_1, \quad \sigma^2 = 1 \longleftrightarrow H_1 : b_0^{(t)} \neq B_0 \quad \text{or} \quad b_1^{(t)} \neq B_1 \quad \text{or} \quad \sigma^2 \neq 1.$$

It is straightforward (see the Appendix) to obtain the generalized likelihood ratio statistic as follows

$$LR_t = \mathrm{C}_t - n\log\widehat{\sigma}_t^2 - n, \tag{6}$$

where

$$\mathrm{C}_t = \sum_{i=1}^{n}(y_{it} - B_0 - B_1x_i^*)^2, \qquad \widehat{\sigma}_t^2 = \frac{1}{n}\sum_{i=1}^{n}(y_{it} - b_{1t}x_i^* - b_{0t})^2,$$

$$b_{0t} = \bar{y}_t, \qquad b_{1t} = \frac{S_{xy(t)}}{S_{xx}}.$$

Subsequently, we incorporate EWMA procedure to the construction of LR_t. Here the EWMA scheme is not to directly average the LR_t statistics but rather to get more precise "estimates" of the current process intercept, slope and variance. To be specific, three EWMA statistics are introduced by

$$\mathrm{EI}_t = \lambda b_{0t} + (1-\lambda)\mathrm{EI}_{t-1},$$
$$\mathrm{ES}_t = \lambda b_{1t} + (1-\lambda)\mathrm{ES}_{t-1},$$
$$\mathrm{EE}_t = \lambda S_t^* + (1-\lambda)\mathrm{EE}_{t-1},$$

where $S_t^* = \frac{1}{n}\sum_{i=1}^{n}(y_{it} - \mathrm{ES}_t x_i^* - \mathrm{EI}_t)^2$, $\mathrm{EI}_0 = B_0$, $\mathrm{ES}_0 = B_1$, $\mathrm{EE}_0 = 1$ and λ is the smoothing parameter satisfying $0 < \lambda < 1$. In general, a smaller λ leads to a quicker detection of smaller shifts (Lucas nad Saccucci, 1990). Note that the moving average estimation of process variance EI_t and ES_t is used in the variance estimation to replace B_0 and B_1. It would be expected to

be more accurate by using these sequentially updated estimations and thus may improve the ability to detect the possible process change. It should be noted that the first term of the statistics LR_t also contains much information about the process, so we introduce another EWMA statistic, as follows:

$$\mathrm{EC}_t = \lambda \mathrm{C}_t + (1-\lambda)\mathrm{EC}_{t-1},$$

where $\mathrm{EC}_0 = n$ as the starting value. Our extensive simulation results verified at this point that the performance of the chart improved significantly.

Finally, substituting EC_t and EE_t for C_t and $\widehat{\sigma}_t^2$ in (6), we obtain the charting statistics

$$ELR_t = \mathrm{EC}_t - n\log \mathrm{EE}_t - n,\ t = 1, 2, \ldots.$$

If $ELR_t > h$, an alarm is trigged, where $h > 0$ is chosen to achieve a specified IC ARL.

Although our method is to use omnibus-type test statistics to implement a single control scheme for detecting shifts in intercept, slope and the variance simultaneously, when the process has gone out of control, we can also obtain some useful information about the process parameters. For example, when an alarm is trigged at point t and at the same time we find that the term EE_t, in the test statistics, deviated from its target significantly, then we can say that the process variance has gone out of control. See more details in the example in Section 5.

3. Adding the VSI performance to the proposed ELR chart

The variable sampling interval (VSI) scheme is a known approach to enhance the efficiency of SPC monitoring schemes. In recent years, several modifications have been suggested to improve traditional fixed sampling rate (FSR) policies that provide better performance than conventional charts in the sense of quicker responses to a process change. Among these, adding VSI in a control chart instead of a fixed sampling interval (FSI) is one of the most popular and useful approaches to improve the detection ability. In a VSI control chart, the sampling interval is varied as a function of the control statistics. The basic idea of the VSI feature is to use a shorter sampling interval if there is an indication of a possible change, but a longer sampling interval if there is no such indication.

Many researchers have contributed to the theory and application of the VSI chart. Most work on developing VSI control charts focuses on monitoring the mean (e.g., Reynolds et al. (1988, 1989, 1990), Runger and Montgomery (1993), Reynolds and Stoumbos (2001) and Reynolds and Amold (2001). Chengular et al. (1989) introduced a VSI Shewhart chart for monitoring the mean and variance with a sample of size of $n > 1$. Reynolds and Stoumbos (2001) added the VSI feature to various combinations of control charts to detect the shift in mean and variance using individual observations. Aparisi (2001) considered a VSI control chart based on Hotelling's statistic. Reynolds and Kim (2005a), and Reynolds and Kim (2005b) recently investigated MEWMA control charts based on sequential sampling and unequal sample size.

Past work on VSI control charts has shown that using only two possible values for the sampling intervals is sufficient. Thus in this article, we consider two possible interval values, say $0 < d_1 < d_2$. To apply the VSI feature to the ELR chart, we apply additional warning limits $0 < \omega < h$ inside the control limits to determine which sampling interval to use next. In particular, a long sampling interval d_2 should be used after the sample is obtained if ELR_t falls inside the warning limits of ω. On the other hand, a short sampling interval d_1 should be used if ELR_t falls outside of the warning limits of ω, but inside the control limits h. If ELR_t falls outside of the control limits, then an out-of-control signal would be triggered. The choices of d_1 and d_2 are determined in practice. When they are determined, then warning limit ω is chosen to achieve a specified IC ATS. In this paper, the warning limit ω is determined through simulation when d_1 and d_2 are fixed.

The speed with which a control chart detects process shifts measures its statistical efficiency. When the interval between samples is fixed, the speed can be measured by ARL. When evaluating the statistical performance of a VSI control chart, the average time to signal (ATS) should be considered. But at the same time, the average number of samples to signal (ANSS) should be considered, too. When a process is in control, it is desirable that the mean time from the beginning of the process until a signal be long, which guarantees fewer false alarms. When a process is out of control, it is desirable that the mean time from the occurrence of the assignable cause until a signal be short, as this guarantees the fast detection of process changes. In the comparative study, we require that all of the charts being compared have the same in-control sampling rate and the same false-alarm rate. This ensures that the charts being compared have the same ATS and ANSS when the process is in-control. When different control charts being compared are designed to have the same IC ATS and ANSS, these charts can be fairly compared according to the steady-state ATS (SSATS). The SSATS is defined as the expected time from the point of the shift to the point at which the chart signals, under the assumption that the control statistic has reached a steady-state distribution by the time that the shift occurs. In this article, we use simulation to approximate the SSATS.

4. Performance comparisons

When evaluating and comparing the performances of static control charts, the ARL performance is considered. This ARL performance is referred to as the zero-state ARL performance. In practice, it may be reasonable to assume that the process starts in control and then shifts at some random time t in the future. For an arbitrarily $t > 0$, the ARL performance of a control chart is called steady-state ARL performance. In this paper, we only tabulate the zero-state ARLs in order to be consistent

Table 1
The ARL comparisons between ELR, MEWMA and KMW chart for the shift in A_0, A_1, standard deviation σ and B_1.

A_0				A_1			
δ	ELR	MEWMA	KMW	δ	ELR	MEWMA	KMW
0.0	200.0	200.0	200.0	0.0	200.0	200.0	200.0
0.1	131.9	131.5	133.7	0.025	99.4	99.0	101.6
0.2	61.2	59.9	59.1	0.0375	58.0	57.4	61.0
0.3	30.8	29.6	28.3	0.05	36.1	35.0	36.5
0.4	18.2	17.2	16.2	0.0625	24.2	23.1	24.6
0.5	12.2	11.5	10.7	0.075	17.3	16.4	17.0
0.6	9.0	8.5	7.9	0.1	10.5	9.8	10.3
0.8	5.8	5.8	5.1	0.125	7.3	6.9	7.2
1.0	4.2	4.1	3.8	0.15	5.5	5.3	5.5
1.5	2.4	2.6	2.4	0.2	3.7	3.7	3.8
2.0	1.6	2.0	1.9	0.25	2.7	2.9	2.9
σ				B_1			
δ	ELR	MEWMA	KMW	δ	ELR	MEWMA	KMW
1.0	200.0	200.0	200.0	0.0	200.0	200.0	200.0
1.1	73.3	76.2	72.8	0.05	120.6	120.5	120.8
1.15	44.0	48.7	48.1	0.075	77.8	77.3	77.3
1.2	28.6	33.2	33.5	0.1	51.2	50.0	49.1
1.25	20.0	24.1	24.9	0.15	25.0	24.0	22.8
1.3	14.9	18.4	19.4	0.2	14.9	14.0	13.1
1.4	9.5	12.1	12.7	0.25	10.1	9.5	8.9
1.6	5.3	7.0	7.2	0.3	7.6	7.1	6.6
1.8	3.7	4.9	5.1	0.4	4.9	4.7	4.4
2.2	2.3	3.1	3.2	0.5	3.6	3.6	3.3
2.6	1.7	2.3	2.5	0.7	2.2	2.5	2.3
3.0	1.5	1.9	2.1	0.9	1.6	2.0	1.9

with Kang and Albin (2000) and Kim et al. (2003). In fact, the steady-state ARLs show similar conclusions (available from the authors), thus they are omitted here.

For simplicity, we only consider the case of overall IC ARL=200. The underlying IC model is the same as that of Kang and Albin (2000) and the parameters in the in-control model are $A_0 = 3, A_1 = 2$ and $\sigma^2 = 1, x_i = 2(2)8$. In Kim et al. (2003), the control limits L_I, L_S and L_E are set to be 3.0156, 3.0109 and 1.3723 for the three EWMA charts, respectively, when the smoothing constant λ is chosen to be 0.2. In the case of known parameters, this design will have an overall IC ARL of roughly 200 and the IC ARL of each chart is about 584.

Note that the monitoring statistics EC_t, EE_t involved in ELR_t do not have an explicit in-control distribution, although b_{0t} and b_{1t} are known to be normally distributed with means B_0 and B_1 and variances σ^2/n and σ^2/S_{xx}, respectively. Because the distribution of ELR_t is quite complicated and there is no direct and simple method to compute the transition matrix for our chart, the ARL results are evaluated by 100,000 Monte Carlo simulations. The methods have been implemented in a FORTRAN program (available from the authors upon request) that uses the routines "rnmvn" "rnnor" and "rnun" to generate multivariate Normal vectors, Normal random variables and Uniform random variables, respectively.

In Zou et al. (2007), the results are obtained through Markov chain approximation. Moreover, the types of shifts considered in this paper are the same as those in Kim et al. (2003), although some other scales, instead of the scale σ, can be used to measure the size of shifts in all parameters.

Next we compare our proposed ELR chart with the KMW chart and the MEWMA chart in terms of OC ARL. The OC ARL's of our proposed ELR chart and those of the KMW chart and the MEWMA chart for detecting the shift in A_0, A_1, σ and B_1 are shown in Table 1. From this table, we observed

- The performance of our proposed ELR chart is comparable for detecting the small and moderate shifts in A_0, A_1 and B_1. For detecting the shifts in A_0 and B_1, the KMW chart does better, and for detecting the shifts in A_1, the MEWMA chart does better. The ELR chart seems a little better than the KMW chart, although the difference is negligible. Note that three monitor statistics $EWMA_I$, $EWMA_S$ and $EWMA_E$ should be compared with three corresponding control limits to detect whether the process has gone out of control in the KMW chart, which is not easier than our ELR chart for practitioners to implement in practice.
- For detecting the shift in standard deviation σ, our proposed ELR chart performs almost uniformly significantly better than the other two charts. This is a very important case in practice because the variance increase means that the quality of the product deteriorates. So it should be detected quickly. This implies that our ELR chart can guard against process and product deterioration quite effectively, which shows the superiority of our ELR chart.

Note that the KMW chart, in detecting the change of standard deviation, is an upper-sided scheme. In Kim et al. (2003), authors suggested using the appropriate methods discussed by Acosta-Mejia et al. (1999) if one wished to detect the decreases in variance. However, our approach can also detect decreases in variance very well. The simulated ARL's are shown in Table 2. For purpose of comparison, we also list the results of the MEWMA chart.

Table 2
The ARL's of the MEWMA and ELR chart for detecting the decrease in variance.

δ	0.10	0.15	0.20	0.25	0.30	0.35	0.40
MEWMA	3.3	3.9	4.5	5.3	6.4	7.8	9.7
ELR	5.6	5.9	5.9	6.0	6.1	6.4	6.9
δ	0.45	0.50	0.55	0.60	0.65	0.70	0.75
MEWMA	12.5	16.5	22.9	33.0	49.1	74.9	114.5
ELR	7.5	8.4	9.5	11.3	14.2	18.9	27.6

Table 3
The ARL comparisons between MEWMA, KMW and ELR chart under combinations of intercept (δ_1) and slope (δ_2) shifts in model (2).

δ_1	δ_2	0.025	0.050	0.075	0.100	0.125	0.150	0.175	0.200	0.225	0.250
0.05	MEWMA	155.8	111.0	72.9	48.0	32.8	23.5	17.7	13.9	11.3	9.5
	KMW	157.6	114.7	74.8	48.3	32.2	22.5	16.9	13.2	10.7	8.9
	ELR	154.8	111.3	73.9	49.0	33.9	24.5	18.6	14.7	12.0	10.0
0.10	MEWMA	118.0	89.2	62.1	42.8	30.2	22.2	16.9	13.5	11.0	9.3
	KMW	122.1	94.6	66.4	44.9	30.7	21.9	16.6	13.1	10.6	8.9
	ELR	118.3	89.7	62.8	43.7	31.3	23.1	17.9	14.2	11.7	9.8
0.15	MEWMA	82.2	66.3	49.5	36.1	26.7	20.2	15.8	12.8	10.6	9.0
	KMW	84.6	70.8	54.5	39.6	28.5	20.9	16.1	12.8	10.4	8.8
	ELR	83.0	67.5	50.6	37.3	27.9	21.1	16.7	13.6	11.3	9.6
0.20	MEWMA	56.4	48.0	38.2	29.6	22.9	18.1	14.5	12.0	10.4	8.8
	KMW	57.1	51.1	42.4	33.3	25.4	19.5	15.4	12.4	10.2	8.7
	ELR	57.0	49.2	39.3	30.7	24.0	18.9	15.3	12.2	9.6	9.0
0.25	MEWMA	39.5	35.0	29.4	24.0	19.5	15.9	13.2	11.2	9.6	8.3
	KMW	39.5	36.5	32.3	27.1	22.0	17.8	14.4	11.9	10.0	8.5
	ELR	39.7	36.2	30.6	25.1	20.4	16.8	13.9	11.7	10.0	8.7
0.30	MEWMA	28.7	26.2	22.9	19.6	16.5	13.9	11.8	10.2	8.8	7.8
	KMW	28.2	26.9	24.7	22.0	18.8	15.7	13.2	11.2	9.6	8.3
	ELR	29.6	27.2	24.1	20.5	17.3	14.7	12.6	10.7	9.4	8.2
0.35	MEWMA	21.7	20.2	18.3	16.1	14.0	12.2	10.6	9.3	8.2	7.3
	KMW	20.9	20.2	19.1	17.6	15.8	13.9	12.1	10.5	9.1	8.0
	ELR	22.5	21.2	19.2	16.9	14.8	12.9	11.2	9.9	8.7	7.7
0.40	MEWMA	17.0	16.1	14.9	13.5	12.0	10.7	9.5	8.5	7.6	6.9
	KMW	16.2	15.9	15.3	14.5	13.5	12.1	10.9	9.7	8.6	7.6
	ELR	17.8	16.9	15.7	14.2	12.7	11.4	10.1	9.0	8.1	7.2
0.45	MEWMA	13.7	13.2	12.4	11.4	10.5	9.5	8.6	7.8	7.1	6.5
	KMW	13.1	12.9	12.6	12.1	11.4	10.6	9.8	8.9	8.0	7.3
	ELR	14.5	13.9	13.1	12.1	11.1	10.0	9.1	8.2	7.5	6.8
0.50	MEWMA	11.4	11.1	10.5	9.9	9.2	8.5	7.8	7.2	6.6	6.1
	KMW	10.8	10.8	10.6	10.3	9.9	9.3	8.7	8.1	7.5	6.9
	ELR	12.1	11.7	11.2	10.3	9.7	8.9	8.2	7.5	6.9	6.3

From Table 2, we can see that for detecting small and moderate decrease in variance, our ELR chart performs significantly better than the MEWMA chart. For example, when $\delta = 0.75$, the OC ARL for the MEWMA chart is 114.5, but for the ELR chart, the OC ARL reduce to 27.8. For very large shifts (e.g., $\delta < 0.3$), the MEWMA chart works better. Note that it is the small to moderate shifts that are difficult to detect for any control chart. We do not think the little inferior position relative to MEWMA chart when detecting large shifts will hamper the use of our ELR chart in practice.

Simultaneous shifts in the intercept and slope in model (2) are also considered in this paper. The OC ARL values are obtained and summarized in Table 3. The magnitudes of shifts in intercept (B_0) and slope (B_1) are consistent with Kim et al. (2003). In general, it seems that the MEWMA chart performs better than the other two charts in most of the cases, but the difference is not very significant. For the ELR and KMW charts, the ELR chart performs almost always better than the KMW chart, especially when the shifts in intercept and slope are both small (e.g., $\delta_1 \leq 0.25$ and $\delta_2 \leq 0.075$) or both moderate and large (e.g., $\delta_1 \geq 0.2$ and $\delta_2 \geq 0.075$).

As mentioned in the last section, when comparing the performance of VSI control charts, ARL is not a proper criterion any more. So, we demonstrate the improved performance in terms of SSATS gained by adding the VSI feature to the ELR chart. Table 4 presents the SSATS values of the VSI and FSI ELR charts for the linear profiles model (1) by 100,000 simulations. The shifts in intercept, slope and standard deviation are investigated. The IC ATS and ANSS of each chart are both set to 200; that is, the average IC sampling rate of the VSI chart is 1 sample per unit time. The numerical results are given in Table 4. Zou et al. (2007) also considered the VSI MEWMA charts for the shifts in intercept and standard deviation. The results are tabulated in parentheses.

From Table 4, we conclude that adding the VSI feature can provide quite substantial reductions in the time required to detect small and moderate shifts. The results presented here, are fairly consistent with previous research on univariate VSI control charts. In general, the interval d_1, should be as small as possible for better statistical performance (Reynolds et al.,

Table 4
SSATS comparisons between FSI ELR and VSI ELR charts for the shift in intercept A_0, slope B_1, A_1 and standard deviation σ.

A_0				A_1			
δ	FSI	$d_1 = 0.5$ $d_2 = 1.25$	$d_1 = 0.1$ $d_2 = 1.9$	δ	FSI	$d_1 = 0.5$ $d_2 = 1.25$	$d_1 = 0.1$ $d_2 = 1.9$
0.1	126.4 (127.9)	122.8(124.4)	112.2(120.0)	0.025	96.0	90.4	80.8
0.2	57.7 (57.6)	52.1 (51.9)	44.2 (45.2)	0.0375	55.6	49.5	41.5
0.3	28.6 (28.1)	23.9 (23.3)	18.0 (18.1)	0.05	33.9	28.5	22.2
0.4	16.5 (16.1)	13.1 (12.6)	9.2 (9.2)	0.0625	22.3	18.0	13.1
0.5	11.0 (10.6)	8.4 (8.0)	5.7 (5.8)	0.075	15.7	12.3	8.6
0.6	8.0 (7.6)	6.0 (5.7)	4.2 (4.2)	0.1	9.4	7.1	4.9
0.8	5.1 (4.8)	3.8 (3.6)	2.8 (2.8)	0.125	6.4	4.8	3.5
1.0	3.7 (3.4)	2.8 (2.6)	2.2 (2.1)	0.15	4.9	3.7	2.7
1.5	2.1 (2.0)	1.6 (1.6)	1.4 (1.4)	0.2	3.2	2.4	2.0
2.0	1.4 (1.4)	1.0 (1.1)	0.9 (1.1)	0.25	2.4	1.8	1.6
3.0	1.0 (0.8)	0.5 (0.8)	0.5 (0.9)	0.3	1.8	1.4	1.2
σ				B_1			
δ	FSI	$d_1 = 0.5$ $d_2 = 1.25$	$d_1 = 0.1$ $d_2 = 1.9$	δ	FSI	$d_1 = 0.5$ $d_2 = 1.25$	$d_1 = 0.1$ $d_2 = 1.9$
0.1	4.4 (2.7)	3.5 (2.1)	2.8 (1.8)	0.05	116.3	111.7	102.7
0.3	5.0 (5.8)	3.9 (4.3)	3.0 (3.3)	0.075	74.2	68.7	60.1
0.5	7.0 (15.9)	5.2 (11.2)	3.7 (7.1)	0.1	48.3	43.2	35.4
0.7	16.8 (73.8)	12.1 (63.9)	7.2 (51.1)	0.15	23.2	19.0	13.9
1.1	70.9 (73.2)	68.3 (68.9)	63.6 (63.9)	0.2	13.5	10.4	7.2
1.2	27.0 (31.2)	24.1(27.4)	20.7 (23.4)	0.25	9.0	6.8	4.8
1.4	8.7 (16.9)	7.1 (14.1)	5.6 (11.4)	0.3	6.7	5.0	3.6
1.8	3.3 (10.8)	2.6 (8.8)	2.2 (6.9)	0.4	4.3	3.3	2.5
2.2	2.1 (4.0)	1.6 (3.2)	1.4 (2.6)	0.5	3.1	2.4	1.9
2.6	1.6 (2.4)	1.1 (1.9)	1.1 (1.7)	0.7	2.0	1.5	1.4
3.0	1.4 (1.3)	0.9 (1.1)	0.9 (1.2)	0.9	1.	0.9	0.9

Table 5
The data set of the example from an optical imaging system.

t	x_1	x_2	x_3	y_1	y_2	y_3
1	0.76	3.29	8.89	1.12	3.49	9.11
2	0.76	3.29	8.89	0.99	3.53	8.89
3	0.76	3.29	8.89	1.05	3.46	9.02
4	0.76	3.29	8.89	0.76	3.75	9.30
5	0.76	3.29	8.89	0.96	3.53	9.05
6	0.76	3.29	8.89	1.03	3.52	9.02

1990); therefore, it usually depends on how soon it is feasible to sample again after the current sample was obtained. On the other hand, the sampling interval d_2, should be chosen to be long so that the resulting control chart would have an acceptable average sampling rate. When compared with VSI MEWMA chart for detecting intercept shifts, our ELR chart has comparable performance. But for variance shifts, our ELR chart shows much superiority. For example, when $\delta = 0.7$, our ELR chart has SSATS 12.1 and 7.2 while VSI MEWMA chart has SSATS 63.9 and 51.1 for $d_1 = 0.5, d_2 = 1.25$ and $d_1 = 0.1, d_2 = 1.9$, respectively. Similar conclusions can be obtained for other types of changes as well.

5. A real data example

In this section, the application of our proposed ELR chart for monitoring linear profiles is illustrated by a real data example Gupta et al. (2006) used to compare the performance of two phase II monitoring schemes for linear profiles, the control charting schemes proposed by Croarkin and Varner (1982) and Kim et al. (2003). The data set consists of line widths of photo masks reference standards on 10 units (40 measurements) used for monitoring linear calibration profiles of an optical imaging system. The line widths are used to estimate the parameters of the linear calibration profile, $y_{it} = 0.2817 + 0.9767x_i$, with a residual standard deviation of 0.06826 micrometers. Interested readers are referred to the NIST/SEMATECH e-Handbook of statistical methods and Gupta et al. (2006) for deeper background.

In Gupta et al. (2006), the in-control ARL is set to 200. Although we have made a detailed comparative study in the last section, we set the same in-control ARL with Gupta et al. (2006) for our proposed ELR chart for monitoring linear profiles to show the application of our ELR chart more clearly. Table 5 shows the data set taken from Table 7 in Gupta et al. (2006), with label "x_1", "x_2", "x_3", "y_1", "y_2" and "y_3". In order to be consistent with model (2), the original data had been standardized by

$$\frac{y_{it}}{0.06826} = \left(\frac{0.2817}{0.06826} + \frac{0.9767}{0.06826}\bar{x}\right) + \frac{0.9767}{0.06826}x_i^* + \varepsilon_{it},$$

Table 6
The statistics results of the example from an optical imaging system.

t	x_1^*	x_2^*	x_3^*	y_1^*	y_2^*	y_3^*	EI_t	ES_t	EE_t	EC_t	ELR_t
1	11.134	48.198	130.237	16.408	51.128	133.460	66.075	14.309	1.123	3.705	0.357
2	11.134	48.198	130.237	14.503	51.714	130.273	65.957	14.309	1.031	3.304	0.231
3	11.134	48.198	130.237	15.328	50.689	132.142	65.980	14.326	0.881	2.857	0.236
4	11.134	48.198	130.237	11.134	54.937	136.244	66.272	14.510	3.231	12.897	6.379
5	11.134	48.198	130.237	14.064	51.714	132.581	66.241	14.519	2.616	10.859	4.974
6	11.134	48.198	130.237	15.089	51.508	132.142	66.246	14.494	2.115	8.848	3.600

where $\varepsilon_{it} \sim N(0, 1)$. Table 6 shows the standardized data with label "x_1^*", "x_2^*", "x_3^*", "y_1^*", "y_2^*" and "y_3^*", where $x_i^* = x_i - \bar{x}$, $y_i^* = 14.6498 y_i$. Some other statistics results with label "EI_t", "ES_t","EE_t", "EC_t" and "ELR_t" are also listed in this table. Here, the in-control model is $y_{it}^* = 65.8443 + 14.3085 x_i^* + \varepsilon_{it}$. Note that the control limit h is 1.752 to achieve in-control ARL 200 when λ is chosen to be 0.2. From Table 6, we can observe our ELR chart gives an out-of-control signal at observation 4. Note that the EE_4 statistics is 3.231, which deviated from its target value 1 significantly, so we can say that the process variance has gone out of control and the variance increased. These results are consistent with those of Gupta et al. (2006). Moreover, this signal is significant enough to show that the process has gone out of control. It is urgent for practitioners to take effective measures. This, again, shows that our ELR chart is quite a useful tool for practitioners.

6. Conclusions and considerations

In this paper, we propose a new method for detecting shifts in intercept, slope and standard deviation for the linear profiles by using a single chart. The proposed scheme integrates the EWMA procedure with the generalized likelihood ratio statistics. The new chart can be easily designed and constructed. By the simulations, we show that the ELR chart performs similarly to the existing charts in terms of OC ARL. For detecting the standard deviation, our proposed new chart works significantly better than the existing competitive charts.

As Kim et al. (2003) pointed out, it is very necessary to justify which parameter or parameters have shifted after a signal occurs. Since their proposed chart is the combination of the three EWMA charts, and each chart detects the corresponding parameter, the diagnosis of any process change is easier than that of the omnibus methods of Kang and Albin (2000). It should be noted that our proposed method is an omnibus chart, but when the process has gone out of control, we also can observe some useful information from the statistics results, about which parameter has shifted. So it is still an advantage of our new chart for practitioners. Of course, for this type of control chart, some diagnostic aids have been proposed and developed in the literature. For example, Hawkins and Zamba (2005) used two conventional parametric tests: a two-sided F test for detecting the changes in variance and an approximate t-test for detecting the changes in mean. So these methods also can be used to diagnose the change of the process.

Acknowledgments

The authors gratefully acknowledge the constructive comments of a co-editor and two anonymous referees that are very helpful for the improvement of this paper. This research is supported by the NSF of Tianjin Grant 07JCYBJC04300, the NNSF of China Grant 10771107 and 10711120448.

Appendix

The derivation of Eq. (6):
As

$$y_{it} - B_0 - B_1 x_i^* = \varepsilon_{it} \sim N(0, 1), \quad i = 1, 2, \ldots, n,$$

then the Log likelihood function under H_0 is

$$l_0 = -\frac{n}{2}\log 2\pi - \frac{\sum_{i=1}^{n}(y_{it} - B_1 x_i^* - B_0)^2}{2}.$$

When we get n samples, the MLE of the parameters are

$$\hat{B_0} = \bar{y}_t, \qquad \hat{B_1} = \frac{S_{xy(t)}}{S_{xx}}, \qquad \hat{\sigma}_t^2 = \frac{1}{n}\sum_{i=1}^{n}(y_{it} - \hat{B_1} x_i^* - \hat{B_0})^2,$$

respectively, then the Log likelihood function under H_1 is

$$l_1 = -\frac{n}{2}\log 2\pi\hat{\sigma}_t^2 - \frac{n}{2}.$$

Then we have the LR_t statistics as follows:

$$-2(l_0 - l_1) = \sum_{i=1}^{n} (y_{it} - B_1 x_i^* - B_0)^2 - n \log \widehat{\sigma}_t^2 - n.$$

References

Acosta-Mejia, C.A., Pignatiello, J.J., Rao, B.V., 1999. A comparison of control charting procedures for monitoring process dispersion. IIE Trans. 31, 569–579.

Aparisi, F., 2001. Hotelling's T^2 control chart with variable sampling intervals. Int. J. Prod. Res. 39, 3127–3140.

Chengular, I.N., Amold, J.C., Reynolds Jr., M.R., 1989. Variable sampling interval for multivariate Shewhart charts. Comm. Statist. Part A-Theory Methods 18, 1769–1792.

Croarkin, C., Varner, R., 1982. Measurement assurance for dimensional measurements on integrated-circuit photomasks. NBS Technical Note 1164, U.S. Department of Commerce, Washington, D.C., USA..

Gupta, S., Montgomery, D.C., Woodall, W.H., 2006. Performance evaluation of two methods for online monitoring of linear calibration profiles. Int. J. Prod. Res. 44, 1937–1942.

Hawkins, D.M., Zamba, K.D., 2005. Statistical process control for shifts in mean or variance using a change-point formulation. Technometrics 47, 164–173.

Jensen, W.A., Brich, J.B., Woodall, W.H., 2008. Monitoring correlation within linear profiles using mixed models. J. Qual. Tech. 40, 167–183.

Kang, L., Albin, S.L., 2000. On-line monitoring when the process yields a linear profile. J. Qual. Tech. 32, 418–426.

Kim, K., Mahmoud, M.A., Woodall, W.H., 2003. On the monitoring of linear profiles. J. Qual. Tech. 35, 317–328.

Lawless, J.F., Mackay, R.J., Robinson, J.A., 1999. Analysis of variation transmission in manufacturing processes-Part I. J. Qual. Tech. 31, 131–142.

Lowry, C.A., Woodall, W.H., Champ, C.W., Rigdon, S.E., 1992. A multivariate EWMA control chart. Technometrics 34, 46–53.

Lucas, J.M., Saccucci, M.S., 1990. Exponentially weighted moving average control schemes: Properties and enhancements.(with discussion). Technometrics 32, 1–29.

Mahmoud, M.A., Woodall, W.H., 2004. Phase I analysis of linear profiles with calibration applications. Technometrics 46, 380–391.

Mahmoud, M.A., Parker, P.A., Woodall, W.H., Hawkins, D.M., 2007. A change point method for linear profile data. Qual. Rel. Eng. Int. 23, 247–268.

Mestek, O., Pavlik, J., Suchanek, M., 1994. Multivariate control charts: control charts for calibration curves. J. Anal. Chem. 350, 344–351.

Prabhu, S.S., Runger, G.G., 1997. Designing a multivariate EWMA control chart. J. Qual. Tech. 29, 8–15.

Reynolds Jr, M.R., Amin, R.W., Arnold, J.C., Nachlas, J.A., 1988. $\bar{X}$ charts with variable sampling intervals. Technometrics 30, 181–192.

Reynolds Jr., M.R., 1989. Optimal variable sampling interval control charts. Sequential Analysis 8, 361–379.

Reynolds Jr., M.R., Amin, R.W., Amold, J.C., 1990. Cusum charts with variable sampling intervals. Technometrics 32, 371–384.

Reynolds Jr., M.R., Amold, J.C., 2001. EWMA control charts with variable sample sizes and variable sampling intervals. IIE Trans. 33, 66–81.

Reynolds, M.R., Kim, K., 2005a. Multivariate monitoring of the process mean with sequential sampling. J. Qual. Tech. 37, 149–162.

Reynolds, M.R., Kim, K., 2005b. Monitoring using an MEWMA control chart with unequal sample sizes. J. Qual. Tech. 37, 267–281.

Reynolds, M.R., Stoumbos, Z.G., 2001. Monitoring process mean and variance using individual observations and variable sampling intervals. J. Qual. Tech. 33, 181–205.

Runger, G.C., Montgomery, D.C., 1993. Adaptive sampling enhancement for Shewhart control charts. IIE Trans. 25, 41–51.

Stover, F.S., Brill, R.V., 1998. Statistical quality control applied to ion chromatography calibrations. J. Chro. A. 804, 37–43.

Williams, J.D., Woodall, W.H., Brich, J.B., 2007. Statistical monitoring of nonlinear product and process quality profiles. Qual. Rel. Eng. Int. 23, 925–941.

Woodall, W.H., 2000. Controversies and contradictions in statistical process control (with discussion). J. Qual. Tech. 32, 341–378.

Woodall, W.H., Spitzner, D.J., Montgomery, D.C., Gupta, S., 2004. Using control charts to monitor process and product quality profiles. J. Qual. Tech. 36, 309–320.

Zou, C., Tsung, F., Wang, Z., 2007. Monitoring general linear profiles using multivariate exponential weighted moving average schemes. Technometrics 49, 395–408.